(Received 4 March 2024, Accepted 27 March 2024, Scheduled 5 April 2024)

A Compact MIMO Antenna with Wideband Charaecteristics for WiFi 6E/X-Band Applications

Janani Sasikumar* and Kanmani Ruby Erode Dhanapal

Vel Tech Rangarajan Dr. Sagunthala R & D Institute of Science and Technology, India

ABSTRACT: A novel proposal for upcoming wireless applications introduces a dual-band, highly decoupled, and compact microstrip patch co-planar waveguide (CPW)-fed MIMO antenna. This low-profile antenna exhibits narrow wide-band performance across the frequency bands of 6.2 to 11.2 GHz, with dimensions of $20 \times 20\,\text{mm}^3$ on a standard FR4 substrate. Through integration onto a printed circuit board (PCB) measuring $20 \times 20\,\text{mm}^2$, the antenna configuration is expanded to a 4×4 MIMO arrangement. Individual antennas within this setup maintain a significant isolation of around 20 dB in the absence of a decoupling mechanism. Fabrication of the designed four-port antenna allows for practical measurement of various antenna parameters. The measured results closely align with simulated outcomes, encompassing S parameters, far-field patterns, and MIMO characteristics such as envelope correlation coefficient, channel capacity loss, and total active reflection coefficient. These results suggest that the antenna design presented in this study holds promise for future wireless applications.

1. INTRODUCTION

The field of wireless communication has seen a steady and continuous expansion since the onset of the 21st century [1]. Industry standards now include notable applications like vehicle-to-vehicle (V2V) communication, driverless cars, and healthcare biomedical systems [2–6]. Contemporary wireless communication is dependent on a range of technologies such as satellite communication, WLAN, global positioning system (GPS), and other relevant wireless applications [3]. In order to optimize the performance of devices, researchers and engineers often include several functionalities into small and smart gadgets [5–11]. Utilizing multi-band antennas prevents interference among different operational frequencies, including streamlining system front-ends [12–18]. One of the familiar methods for obtaining numerous frequency bands is incorporating additional slots into the antenna patch [6]. The slots possess resonance frequencies that are separate from those of the patch, leading to the occurrence of supplementary resonances [19–21]. Recently, fractal geometry has emerged as a novel approach in the design of multi-band patch antennas, offering a range of fractal patterns to achieve superior performance [8]. As time passes, multiple-input multiple-output (MIMO) antenna systems have been created for both single-band and dual-band purposes [22–24]. Specifically, a pair of slot-based multiple-input multiple-output (MIMO) antennas were developed for 4G/5G mobile phones, along with a wideband MIMO antenna for wireless local area network (LAN) applications [25, 26].

These designs exhibit more compactness than conventional patch antennas, although they possess smaller frequency ranges. The use of fractal geometries poses difficulties in achieving precise construction of intricate structures. Hence, the novel study proposes the utilization of a printed dipole to bolster split ring resonators (SRR). This process entails the printing of SRRs directly onto antennas, offering an alternate approach to fabricating patch antennas with multiple resonances. This design incorporates a single antenna that can operate over three different frequency bands, including WLANs and fixed satellite services.

A compact antenna that will operate at the frequency range of 6.2 to 11.2 GHz with four ports is represented. The antenna is separated into four distinct phases. Phase I encompasses the design and construction of the antenna, while Phase II provides comprehensive analysis of simulation findings, such as S-parameters, parametric studies, current distribution, and polarisation diversity. During Phase III, the outcomes are assessed by using a synthetic prototype. Phase IV entails the examination of several MIMO parameters via the use of graphs.

2. DESIGN AND CONFIGURATION OF MIMO ANTENNA

The illustrated antenna for wireless applications, featuring a modified circular design with four ports, is presented in Figure 1. Constructed on a commonly utilized FR4 substrate measuring $20 \times 20\,\text{mm}^2$, the quad-element circular printed antenna incorporates a ground plane on the top side of the substrate, measuring $P2 \times Q2\,\text{mm}^2$, to facilitate antenna fabrication. Positioned above the modified circular radius $R1$, the suggested antenna comprises a feeding element measuring $P4 \times Q4\,\text{mm}^2$ and a truncated rectangular element measuring $P3 \times Q3\,\text{mm}^2$.

For the purpose of achieving the best possible isolation and a wide range of patterns, every antenna is deliberately positioned at one of the four corners of the substrate. The precise building specifications, including measurements, are shown in Fig-

* Corresponding author: Janani Sasikumar (jananiscorptech@gmail.com).

Parameters	$P1$	$Q1$	$P2$	$Q2$	$P3$	$Q3$	$P4$	$Q4$
Values (mm)	20	20	1.98	3.47	1.05	2.35	1.05	3.58

TABLE 1. Various parameters of the proposed antenna.

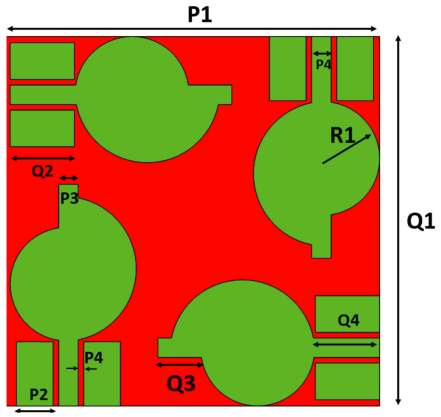

FIGURE 1. Structure and dimension of the proposed antenna.

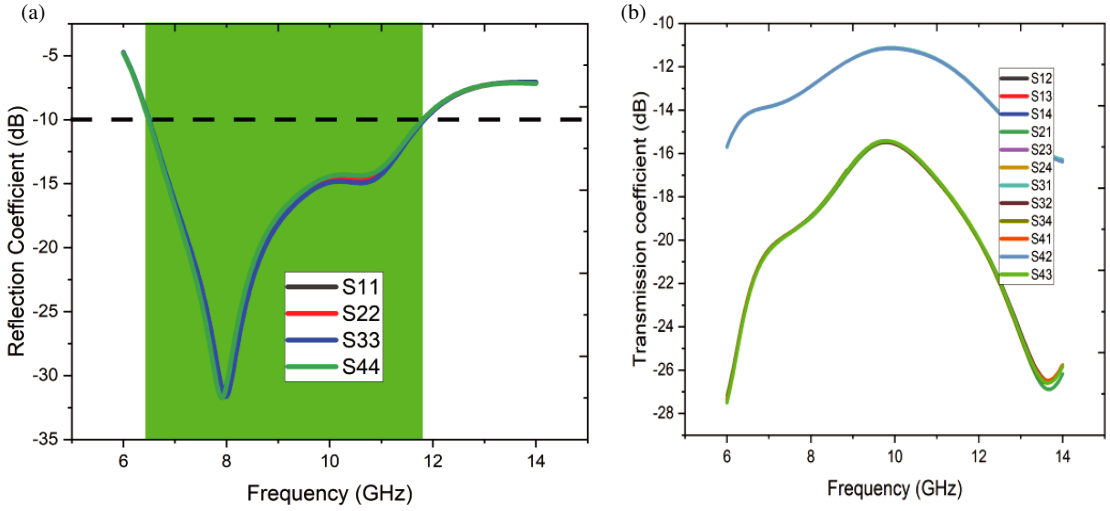

FIGURE 2. (a) Reflection coefficient, (b) transmission coefficient of the proposed antenna.

ure 1. Table 1 presents the precise measurements for each truncated Wi-Fi 6E antenna element. These measurements are established and unchangeable by parametric analysis conducted using ADS EM-simulator.

Figures 2(a) and (b) display the reflection and transmission coefficients of antennas 1 through 4. Every antenna component in the MIMO system covers a dual band frequency spectrum, as shown in Figure 2(a), with each band spanning a range of frequencies between 6.25 GHz and 11.8 GHz. Conversely, the transmission coefficient of the 4-port antenna arrangement in Figure 2(b). Achieving isolation up to 12.5 dB across antenna systems requires aligning each antenna in an orthogonal manner. The main important fact is that it does not need the decoupling procedure which is another advantage of orthogonal placement.

3. ANALYSIS PARAMETRIC

Figure 1(a) presents the complete structure of designed four-port MIMO antenna system where radiating elements are located in such a way that the antennas radiate their electromagnetic energy orthogonally. Since the designed antenna belongs to CPW family, the ground plane of the antenna is printed on the same surface where antenna is printed. The designed antenna comprises two parts: Feeding element and radiating patch. Feeding strip has the dimension of $(P2 \times Q2)\,\text{mm}^2$ after tuning it to be with the impedance of 50 ohm. The radiating element is in the form of modified circular patch with the radius of R mm. In order to improve the performance in terms of bandwidth and impedance matching, a strip of dimension $(P4 \times Q4)$ mm is designed at the top of 1.97 to 3.47 mm as depicted in Figure 3(a). As can be seen in Figures 3(b) and 3(c), when $Q3$ and $Q4$ are altered, both the lower band responses and higher band responses are severely hampered. Surface current visualisations show the distinctive roles.

According to Figure 4, the surface current distributions illustrate the behaviour at 5.5 GHz and 6.5 GHz when the antenna is excited. It is evident that activating port 1 effectively isolates all other ports from current flow. This improved isolation leads to significant enhancements as observed.

4. MEASURED OUTCOMES AND DISCUSSIONS

Furthermore, to effectively develop the proposed 4-port truncated antenna prototype, real-world testing of the standard antenna characteristics has also been accomplished. The top and

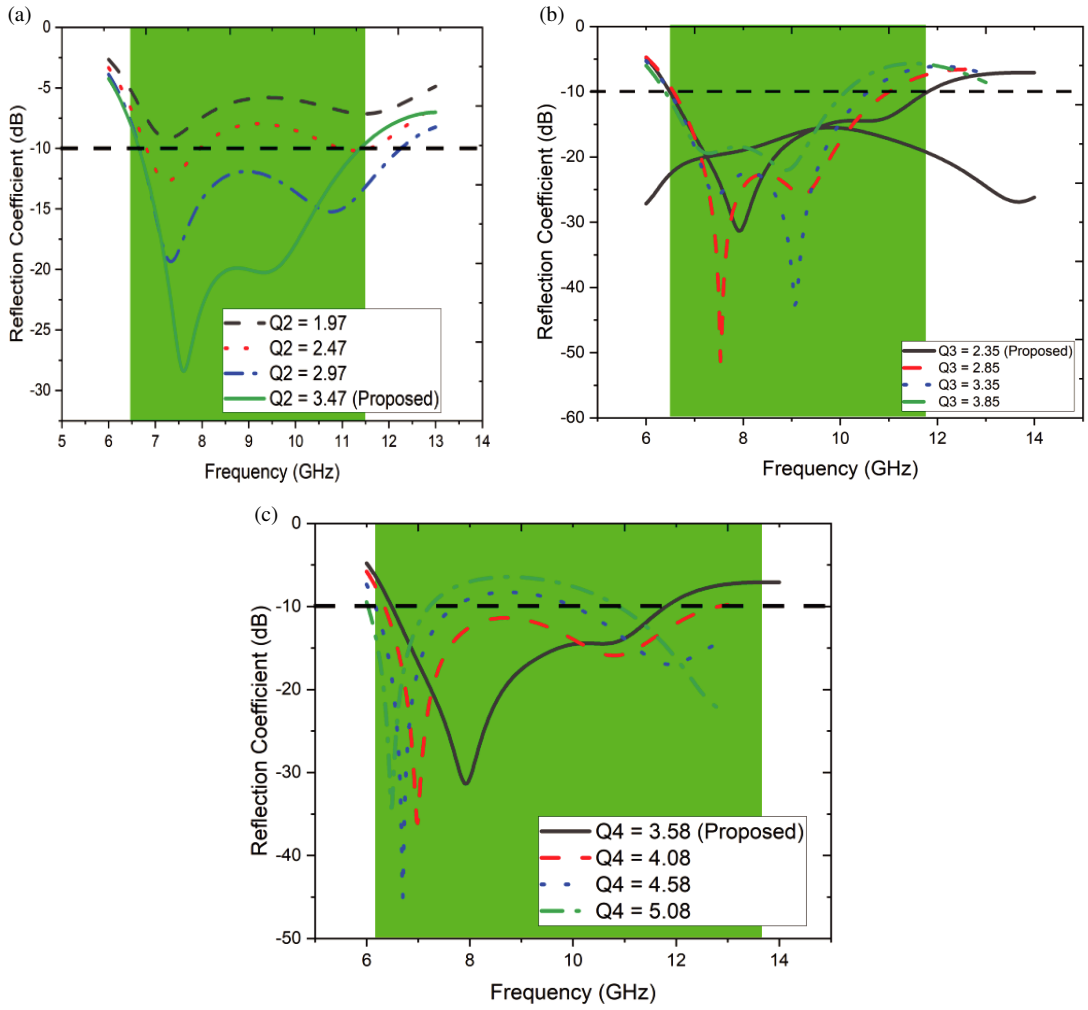

FIGURE 3. Parametric study of the proposed antenna when changing (a) $Q2$, (b) $Q3$, (c) $Q4$.

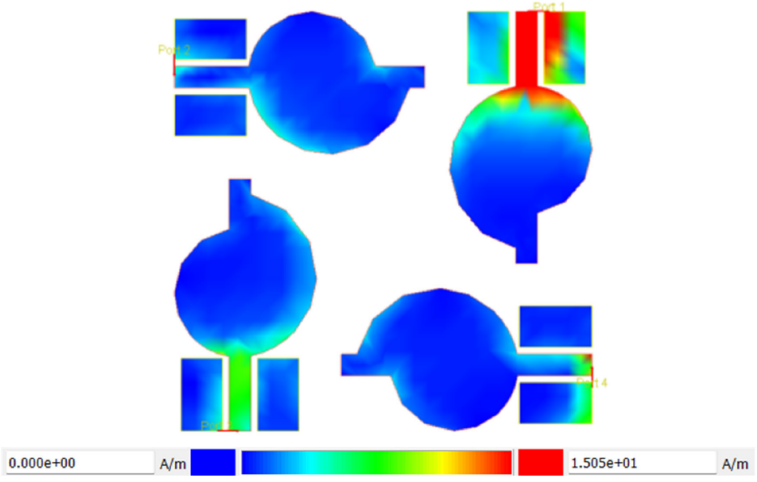

FIGURE 4. Surface current distribution of Antenna 1 at (a) 5.5 GHz, (b) 6.5 GHz.

bottom perspectives of the constructed antenna are shown in Figure 5. Except for the antenna being measured, every SMA connector is terminated with 50 ohms during measurements.

Figures 5(a), (b), and (c) display the S-parameters, also known as reflection and transmission coefficients, which are evaluated with Keysight's Firefox Network Analyzer. It is clear that there is a good correlation between the simulation find-

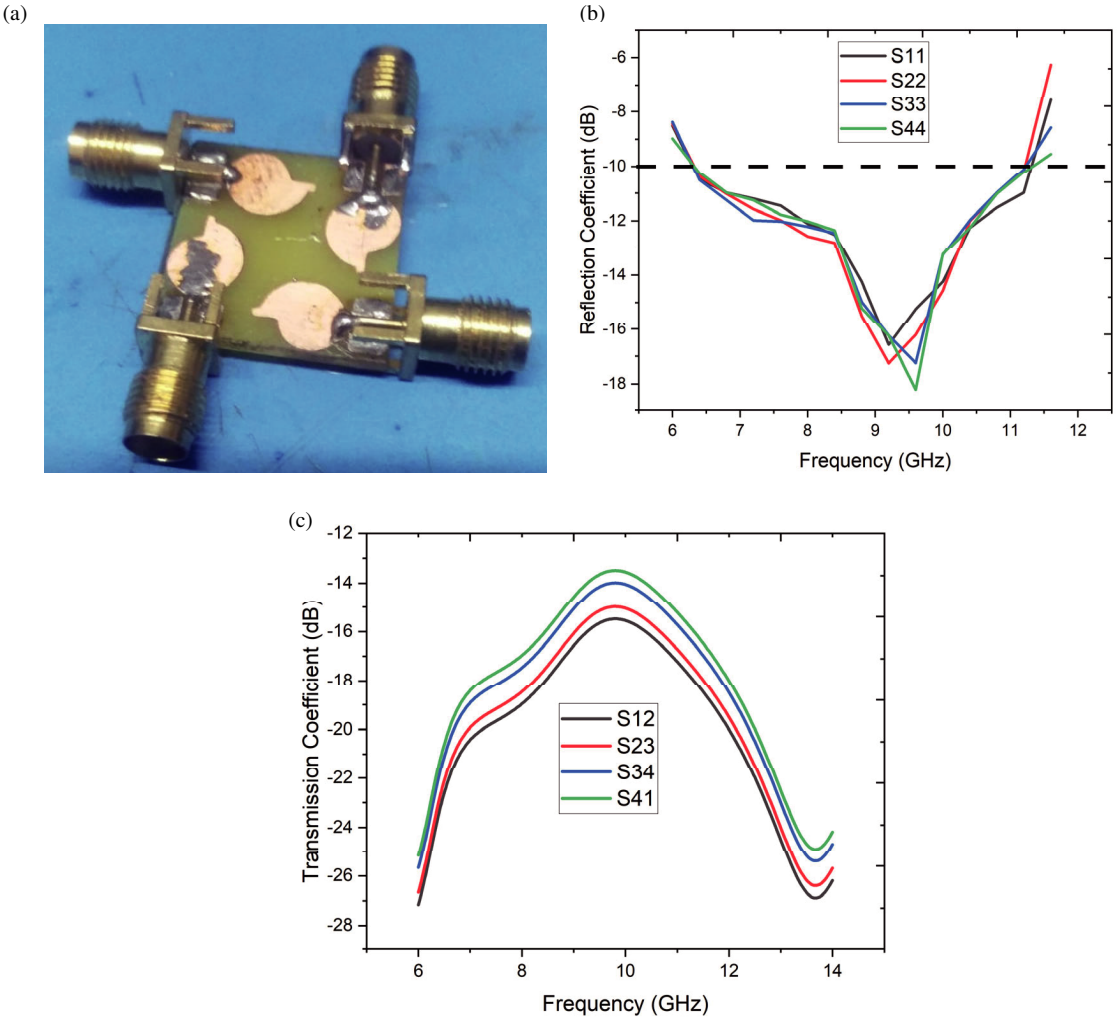

FIGURE 5. (a) Fabricated prototype of MIMO antenna. Measured (b) reflection co-efficient, (c) transmission co-efficient.

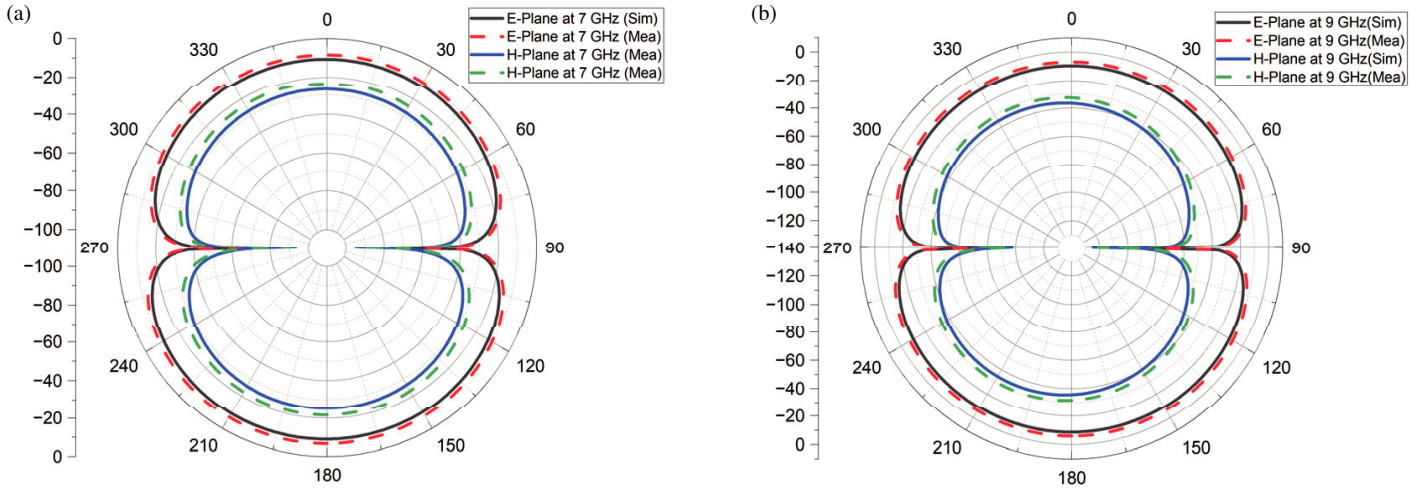

FIGURE 6. Two-dimensional radiation pattern of antenna 1.

ings, which contain two desirable bands of operations, and the measurements. The measurements often show extremely tiny variations, which are attributed to variations in the dielectric constant of the substrate as well as conducting losses caused by soldering effects.

The antenna's two-dimensional radiation pattern at 6.2 GHz and 11.2 GHz for phi = 0° and phi = 90° is shown in Figures 6(a)–(b). The proposed antenna demonstrates cross-polarization of less than 30 dB across the necessary operating bands. Additionally, it produces a co-polarized, bi-directional

TABLE 2. Performance comparison of proposed antenna with literature.

S.No	MIMO antenna size	MIMO antenna size in terms of wavelength (λ)	Individual antenna size (mm^2)	Individual antenna size in terms of wavelength (λ)	Isolation (dB)	Operating Frequency (GHz)	ECC	Gain (dB)
[11]	60×90	$0.49\lambda \times 0.735\lambda$	17×21	$0.138\lambda \times 0.1715\lambda$	18	2.45	NA	0.55
[12]	100×50	$0.816\lambda \times 0.408\lambda$	18×14	$0.147\lambda \times 0.1143\lambda$	10	2.45	NA	NA
[13]	61×61	$0.498\lambda \times 0.498\lambda$	—	—	28	2.45	< 0.3	3.8
[14]	60×60	$0.49\lambda \times 0.498\lambda$	—	—	22	2.45	< 0.4	3.4
[15]	42×42	$0.77\lambda \times 0.77\lambda$	22×16	$\lambda \times 0.293\lambda$	10	5.5	NA	5
[16]	140×120	$1.09\lambda \times 0.94\lambda$	15.5×8	$0.121\lambda \times 0.062\lambda$	15	2.35	NA	NA
[18]	40×40	$0.446\lambda \times 0.446\lambda$	27×18	$0.3015\lambda \times 0.201\lambda$	10	3.35	NA	7.9
[19]	50×50	$0.408\lambda \times 0.408\lambda$	—	—	17.5	2.45	< 0.5	2.1
[20]	100×60	$0.703\lambda \times 0.422\lambda$	15×8	$0.1055\lambda \times 0.056\lambda$	NA	2.119 & 17.55	0.04	8
[21]	60×60	$0.49\lambda \times 0.49\lambda$	22×17	$0.179\lambda \times 0.138\lambda$	17	0.875, 1.75, 1.822, 2.45	< 0.05	-2
[22]	52×52	$0.676\lambda \times 0.676\lambda$	20×20	$0.26\lambda \times 0.26\lambda$	20	3.4 & 3.9	< 0.5	6
[26]	25×25	$0.54\lambda \times 0.54\lambda$	10.485×7.5	$0.22\lambda \times 0.1625\lambda$	25	5.5 & 6.5	< 0.1	2.2–2.5
This Work	20×20	$0.73\lambda \times 0.73\lambda$	5.625×12	$0.20625\lambda \times 0.44\lambda$	20	6–11.5	< 0.1	3.5–7

radiation pattern during resonance. Furthermore, a high correlation is shown between the measured and modelled patterns. Figure 7 illustrates the antenna's gain, ranging from approximately 3.8 to 7 dB across the operational bandwidth. This underscores the suitability of the recommended antenna for future 6E wireless applications.

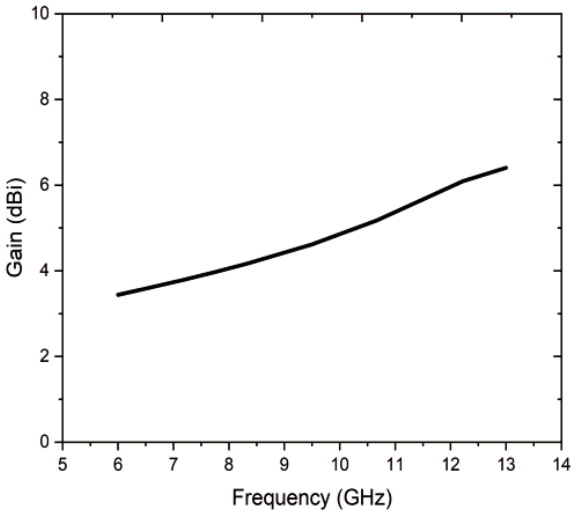

FIGURE 7. Gain of the proposed antenna.

5. THE PERFORMANCE OF MIMO

In a communication system with multiple channels, the performance of a MIMO antenna in terms of envelope correlation coefficient (ECC) is an important statistic to use when determining how isolated one channel is from the others. In MIMO, the antenna works better when the value is lower. The ECCs are generated by utilising Equation (1) and the observed S-parameters to assess the performance of the proposed MIMO antenna.

$$\mathrm{ECC} = \frac{|Saa^* Sab + Sba^* Sbb|^2}{\left(1 - |Saa|^2 - |\mathrm{Sab}|^2\right)\left(1 - |Sba|^2 - |Sbb|^2\right)} \quad (1)$$

Every acceptable frequency range has an ECC value less than 0.035 as in Figure 8(a), suggesting that the overall performance is fairly good. The diversity scenario provided by a MIMO antenna can help improve the signal-to-noise ratio (SNR) of the system over that of a single antenna. One statistic that can be used to determine how much the signal-to-noise ratio has improved is the diversity gain (DG). The question of how to find the outcome of DG's computation using ECC is answered by Equation (2) and illustrated in Figure 8(b)

$$\text{Diversity Gain}\,(c,d) = \sqrt{1 - \mathrm{ECC}_{c,d}} \quad (2)$$

Furthermore, we examine the MIMO antenna's channel capacity loss, or CCL as it is commonly known. Equation (3) is used to calculate CCL, a crucial data transmission rate metric, mathematically.

$$\text{Channel Loss}\,(\mathrm{CL}) = -\log_2 \det\left(\varphi^R\right) \quad (3)$$

$$\varphi^R = \begin{bmatrix} p_{11} & \cdots & p_{14} \\ \vdots & \ddots & \vdots \\ p_{41} & \cdots & p_{44} \end{bmatrix} \quad (4)$$

where,

$$p_{cc} = 1 - \left(\left(S_{cc}^2\right) + \left(S_{cd}^2\right)\right)$$
$$p_{ij} = -\left(S_{cc}^* S_{cd} + S_{dc}^* S_{dd}\right) \quad \text{for } c, d = 1, 2 \ldots 4$$

The desirable CCL value of less than 0.4 bits/sec/Hz is maintained as in Figure 8(c), which is considerable along with the

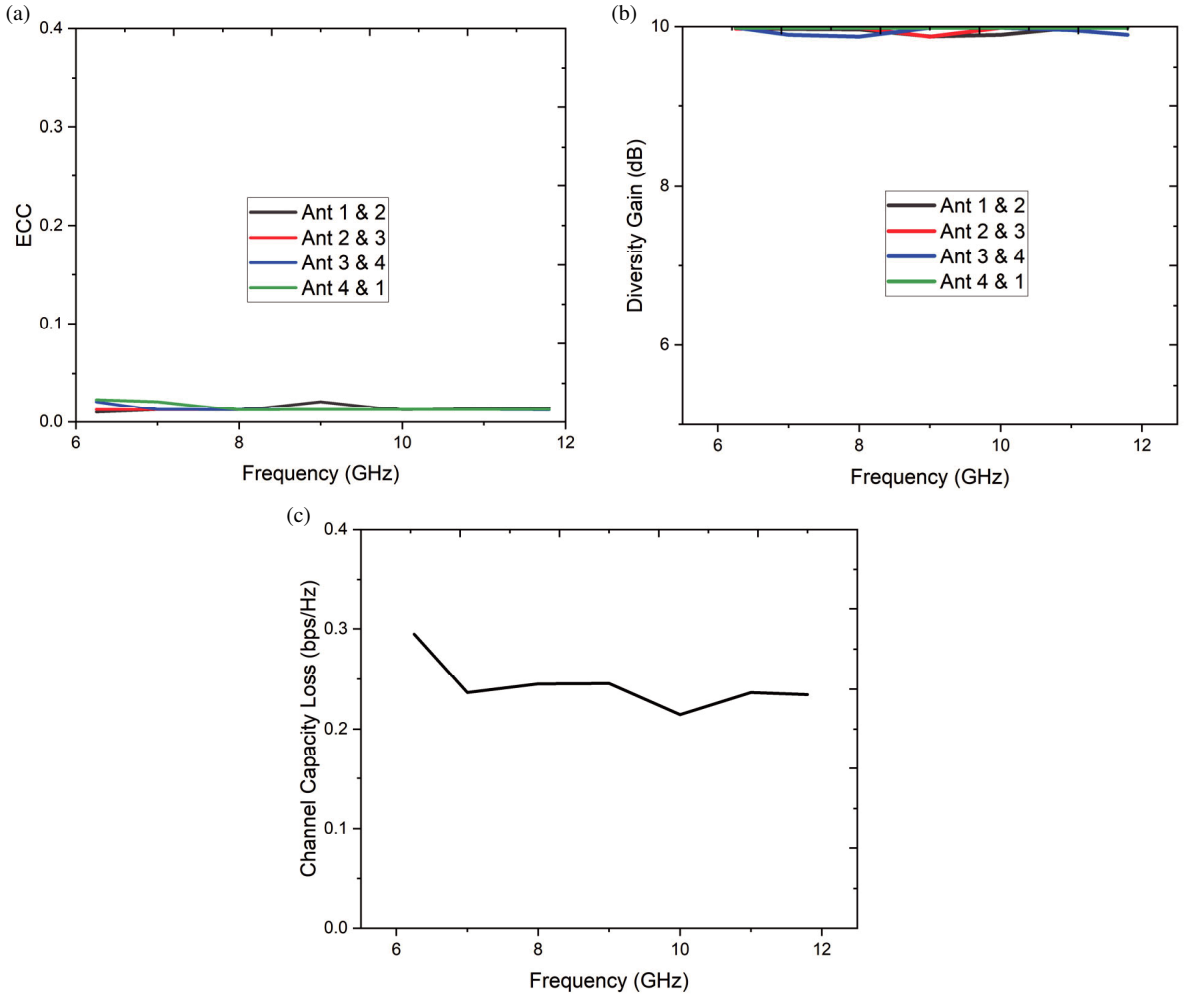

FIGURE 8. MIMO parameters (a) ECC, (b) diversity gain, (c) CCL.

CCL simulations and guarantees sufficient data rate transmission in MIMO systems. The actual and expected channel capacity for the proposed antenna is obtained. However, MIMO performance is the basic step in calculating the channel capacity. Because SNR of the environment is 20 dB, the channel capacity has been calculated usingantenna elements with the stimulated efficiency. The ideal 4×4 MIMO antenna has a channel capacity around 22.28 bps/Hz, while the ideal single-input, single-output antenna has a channel capacity about 5.57 bps/Hz. To sum up, it is evident that the suggested antenna performs better than all of the important MIMO requirements, such as channel capacity, DG, CCL, and ECC.

Table 2 provides performance comparison of the proposed work with other works in literature. In comparison to other configurations listed, the proposed work stands out for its compact size, measuring 20×20. Despite its smaller dimensions, it maintains a remarkable isolation of 20 dB, effectively minimizing interference between antennas. Operating within the frequency range of 6 GHz to 11.5 GHz, it covers a wide spectrum suitable for diverse applications. Additionally, the proposed work achieves an Envelope Correlation Coefficient (ECC) of less than 0.1, indicating minimal correlation between antennas and ensuring robust signal diversity. Its gain, ranging from 3.5 dB to 7 dB, ensures strong signal reception. Overall, the proposed design presents a compelling combination of compact size, excellent isolation, wide frequency coverage, low correlation, and strong signal reception, making it a promising choice for various MIMO antenna applications.

6. CONCLUSION

In summary, the proposed novel wireless application introduces a dual-band, highly decoupled, and compact microstrip patch co-planar waveguide (CPW)-fed MIMO antenna. This antenna, with dimensions of $20 \times 20\,\text{mm}^2$ on a standard FR4 substrate, showcases narrow wide-band performance spanning the frequency bands of 6.2 to 11.2 GHz. When being integrated onto a $20 \times 20\,\text{mm}^2$ printed circuit board (PCB), the antenna configuration expands to a 4×4 MIMO arrangement, while maintaining significant isolation of around 20 dB between individual antennas. Fabrication of the designed four-port antenna enables practical measurement of various antenna parameters, with measured results closely aligning with simulated outcomes across S parameters, far-field patterns, and MIMO characteristics. The promising performance exhibited by this antenna design suggests its potential for shaping the landscape of future wireless applications.

REFERENCES

[1] Kuo, Y.-L. and K.-L. Wong, "Printed double-T monopole antenna for 2.4/5.2 GHz dual-band WLAN operations," *IEEE Transactions on Antennas and Propagation*, Vol. 51, No. 9, 2187–2192, 2003.

[2] Liu, W.-C., W.-R. Chen, and C.-M. Wu, "Printed double S-shaped monopole antenna for wideband and multiband operation of wireless communications," *IEE Proceedings — Microwaves, Antennas and Propagation*, Vol. 151, No. 6, 473–476, 2004.

[3] Ammann, M. and R. Farrell, "Dual-band monopole antenna with stagger-tuned arms for broadbanding," in *2005 IEEE International Workshop on Antenna Technology, IWAT 2005*, 278–281, 2005.

[4] John, M. and M. J. Ammann, "Integrated antenna for multiband multi-national wireless combined with GSM1800/PCS1900/IMT2000 + extension," *Microwave and Optical Technology Letters*, Vol. 48, No. 3, 613–615, 2006.

[5] Ge, Y., K. P. Esselle, and T. S. Bird, "Compact triple-arm multiband monopole antenna," in *2006 IEEE International Workshop on Antenna Technology, IWAT 2006*, Vol. 1, 172–175, 2006.

[6] Wang, H., "Dual-resonance monopole antenna with tuning stubs," *IEE Proceedings — Microwaves, Antennas and Propagation*, Vol. 153, No. 4, 395–399, 2006.

[7] Wang, H. and M. Zheng, "Triple-band wireless local area network monopole antenna," *IET Microwaves, Antennas & Propagation*, Vol. 2, No. 4, 367–372, 2008.

[8] Herraiz-Martinez, F. J., G. Zamora, F. Paredes, F. Martin, and J. Bonache, "Multiband printed monopole antennas loaded with OCSRRs for PANs and WLANs," *IEEE Antennas and Wireless Propagation Letters*, Vol. 10, 1528–1531, 2011.

[9] Long, S. and M. Walton, "A dual-frequency stacked circular-disc antenna," *IEEE Transactions on Antennas and Propagation*, Vol. 27, No. 2, 270–273, 1979.

[10] Herraiz-Martinez, F. J., L. E. Garcia-Munoz, D. Gonzalez-Ovejero, V. Gonzalez-Posadas, and D. Segovia-Vargas, "Dual-frequency printed dipole loaded with split ring resonators," *IEEE Antennas and Wireless Propagation Letters*, Vol. 8, 137–140, 2009.

[11] Khan, M. U. and M. S. Sharawi, "Isolation improvement using an MTM inspired structure with a patch based MIMO antenna system," in *The 8th European Conference on Antennas and Propagation (EuCAP 2014)*, 2718–2722, The Hague, Netherlands, 2014.

[12] Sharawi, M. S., M. U. Khan, A. B. Numan, and D. N. Aloi, "A CSRR loaded MIMO antenna system for ISM band operation," *IEEE Transactions on Antennas and Propagation*, Vol. 61, No. 8, 4265–4274, Aug. 2013.

[13] Ramachandran, A., S. Mathew, V. P. Viswanathan, M. Pezholil, and V. Kesavath, "Diversity-based four-port multiple input multiple output antenna loaded with interdigital structure for high isolation," *IET Microwaves, Antennas & Propagation*, Vol. 10, No. 15, 1633–1642, Dec. 2016.

[14] Ramachandran, A., S. V. Pushpakaran, M. Pezholil, and V. Kesavath, "A four-port MIMO antenna using concentric square-ring patches loaded with CSRR for high isolation," *IEEE Antennas and Wireless Propagation Letters*, Vol. 15, 1196–1199, Nov. 2015.

[15] Luo, Y., Q.-X. Chu, J.-F. Li, and Y.-T. Wu, "A planar H-shaped directive antenna and its application in compact MIMO antenna," *IEEE Transactions on Antennas and Propagation*, Vol. 61, No. 9, 4810–4814, Sep. 2013.

[16] Liao, W.-J., C.-Y. Hsieh, B.-Y. Dai, and B.-R. Hsiao, "Inverted-F/slot integrated dual-band four-antenna system for WLAN access points," *IEEE Antennas and Wireless Propagation Letters*, Vol. 14, 847–850, Dec. 2014.

[17] Moradikordalivand, A., T. A. Rahman, and M. Khalily, "Common elements wideband MIMO antenna system for WiFi/LTE access-point applications," *IEEE Antennas and Wireless Propagation Letters*, Vol. 13, 1601–1604, Aug. 2014.

[18] Sonkki, M., D. Pfeil, V. Hovinen, and K. R. Dandekar, "Wideband planar four-element linear antenna array," *IEEE Antennas and Wireless Propagation Letters*, Vol. 13, 1663–1666, Aug. 2014.

[19] Wang, H., L. Liu, Z. Zhang, Y. Li, and Z. Feng, "A wideband compact WLAN/WiMAX MIMO antenna based on dipole with V-shaped ground branch," *IEEE Transactions on Antennas and Propagation*, Vol. 63, No. 5, 2290–2295, May 2015.

[20] Sharawi, M. S., M. Ikram, and A. Shamim, "A two concentric slot loop based connected array MIMO antenna system for 4G/5G terminals," *IEEE Transactions on Antennas and Propagation*, Vol. 65, No. 12, 6679–6686, Dec. 2017.

[21] Kumar, A., A. Q. Ansari, B. K. Kanaujia, and J. Kishor, "High isolation compact four-port MIMO antenna loaded with CSRR for multiband applications," *Frequenz*, Vol. 72, No. 9-10, 415–427, 2018.

[22] Dash, J. C. and D. Sarkar, "A four-port CSRR-loaded dual-band MIMO antenna with suppressed higher order modes," *IEEE Access*, Vol. 10, 30 770–30 778, 2022.

[23] Paz, Montero-de J., E. Ugarte-Munoz, F. J. Herraiz-Martinez, V. Gonzalez-Posadas, L. E. Garcia-Munoz, and D. Segovia-Vargas, "Multifrequency self-diplexed single patch antennas loaded with split ring resonators," *Progress In Electromagnetics Research*, Vol. 113, 47–66, 2011.

[24] Herraiz-Martínez, F. J., F. Paredes, G. Zamora, F. Martin, and J. Bonache, "Dual-band printed dipole antenna loaded with open complementary split-ring resonators for wireless applications," *Microwave and Optical Technology Letters*, Vol. 54, No. 4, 1014–1017, 2012.

[25] Caloz, C., T. Itoh, and A. Rennings, "CRLH metamaterial leaky wave and resonant antennas," *IEEE Antenn. Propag. Mag.*, Vol. 50, No. 5, 25–39, 2008.

[26] Kumar, D. R., T. Sangeetha, K. G. S. Narayan, G. V. Babu, V. Prithivirajan, and M. S. K. Manikandan, "A miniaturized CPW-fed CSRR loaded quad-port MIMO antenna for 5.5/6.5 GHz wireless applications," *International Journal of Microwave and Wireless Technologies*, 1–10, 2023.